Wavelength switchable mode-locked fiber laser with a few-mode fiber filter

Shaokang Bai(白少康), Yujin Xiang(向昱锦), and Zuxing Zhang(张祖兴)†

Advanced Photonic Technology Laboratory, College of Electronic and Optical Engineering, Nanjing University of Posts and Telecommunications, Nanjing 210023, *China*

(Received 16 March 2022; revised manuscript received 18 May 2022; accepted manuscript online 29 May 2022)

We have proposed and constructed a few-mode fiber (FMF)-based comb filter realized by dislocation splicing a few-mode long-period fiber grating (FM-LPFG) with a single-mode fiber (SMF). From an all-fiber laser with a FMF-based comb filter, the generation of switchable single-, dual-, triple-, and quadruple-wavelength continuous light has been achieved. Moreover, wavelength switchable mode-locked pulses have been obtained with the increased pump power. In the experiment, the output wavelength of the mode-locked fiber laser was changed from 1567.72 nm to 1571.04 nm, while the signal-to-noise (SNR) ratio was maintained above 61 dB. The switchable multiwavelength continuous wave (CW) and mode-locked all-fiber lasers have potentially important applications for fiber sensing, wavelength-division multiplexing (WDM) and signal processing.

Keywords: few-mode fiber, mode-locked pulses, few-mode long-period fiber, comb filter

PACS: 42.55.Wd, 42.65.Re, 42.81.Dp, 42.81.–i **DOI:** 10.1088/1674-1056/ac744f

1. Introduction

The application of the fiber laser in fiber sensing,[1,2] microwave photonic systems,[3,4] optical communication,[5,6] and other fields has aroused extensive research interest and has developed rapidly — in particular, multiwavelength continuous wave (CW) lasers and mode-locked fiber lasers with switchable wavelength features, flexible operating wavelength and broad application space. A filter is indispensable for multiwavelength or wavelength switchable fiber lasers. Being perfectly compatible with fiber lasers and retaining the compactness of the fiber lasers, the all-fiber filter is more desirable, mainly including the fiber grating filter, the Sagnac comb filter, the Mach–Zehnder interferometry (MZI) fiber filter, the few-mode fiber (FMF) filter, and so on. Multi-wavelength lasers based on fiber gratings, such as fiber Bragg gratings (FBGs) written in birefringent fibers[7] — the combination of FBGs and arrayed waveguide gratings,[8] etc. — are simple in structure and easy to use in lasers. However, the number of output wavelengths depends on the number of used fiber gratings. When more wavelengths need to be realized, a large number of FBGs will increase the loss and complexity of the system. Fiber lasers using Sagnac comb filters to form multiple wavelengths have also been reported. Hu *et al*.[9] demonstrated a random combination of a three wavelengths fiber laser based on a multisection high-birefringence fiber filter. In 2020, an LP_{11} mode output multiwavelength fiber laser based on dual Sagnac comb filters was realized.[10] The filter consists of three optical couplers, two polarization controllers (PCs) and two sections of polarization-maintaining fibers to achieve a stable five wavelengths output. Although this filter can achieve stable multi-wavelength lasers in lasers, the structure usually requires two PCs and special high-birefringence fibers. This is detrimental to the compactness and practicality of fiber lasers. Comb fiber filters based on MZI have also received extensive attention. Sierra-Hernandez *et al*. demonstrated a MZI based single-mode fiber (SMF)-photonic crystal fiber (PCF)-SMF filter structure to realize single-, dual-, and triple-wavelength switchable erbium-doped fiber (EDF) lasers through controlling the curvature radius of the MZI,[11] with a tunable spectral range of 26 nm. Feng *et al*. realized a switchable multiwavelength EDF laser based on MZI using a dual-core fiber as a comb filter, achieving a maximum three wavelengths output.[12] The MZI structure formed by using a PCF or dual-core fiber has large loss, and the multiwavelength excitation in the laser is limited. In addition, an MZI structure based on an acoustic controlled etched SMF has been studied, realizing a fast-tuning dual-wavelength fiber laser with a spacing of about 3.5 nm.[13] Although there is some flexibility in using acoustic waves to control wavelengths, the structure is difficult to fabricate and inconvenient to apply.

Recently, fiber filters based on FMFs have also been intensely investigated. Zou *et al*. reported a tunable self-seeded multiwavelength Brillouin-erbium fiber laser based on a FMF filter, where the FMF filter was fabricated by splicing a 5.0-cm-long FMF between two up-tapers.[14] The free spectral range (FSR) of such a FMF filter is cumbersome to tune and is highly dependent on room temperature. Qi *et al*. proposed a FMF filter based on a core-shifted structure, realizing a fiber laser of up to four wavelengths.[15] Tang *et al*. also realized the continuous generation of a wavelength-switchable LP_{11}

†Corresponding author. E-mail: zxzhang@njupt.edu.cn

© 2023 Chinese Physical Society and IOP Publishing Ltd

mode all-fiber laser based on a FMF filter of the SMF–FMF–SMF structure.[16] However, for the FMF filter composed of SMF–FMF–SMF, the formation of the interference spectrum requires the perfect matching of the two dislocation splicing points. Recently, Liu *et al*. proposed a comb filter spectral structure formed by cascading two mode-selective couplers (MSCs) with a FMF,[17] and stated that the operating bandwidth of the filter is related to the distance of the coupling arms, and the FSR correlates with the length of the two interference arms. This structure has the function of both mode selection and wavelength selection. However, this structure has high requirements on the performance of the MSC, which increases the difficulty of fabrication.

In this paper, we utilize a dislocation splicing between a few-mode long-period fiber grating (FM-LPFG) and a SMF to form a simple FMF comb filter structure. The FSR of the FMF filter (FMFF) is related to the length of the FMF. Leveraging the FMF filter with a FSR of 3.2 nm, an extinction ratio of 9 dB and a loss of 3 dB, switchable single-, dual-, triple-, and quadruple-wavelength CW laser outputs have been realized. After increasing the pump power, a stable soliton pulse output can also be achieved, and the wavelength of the pulsed laser can be switched. Compared with the reported traditional filtering structure based on a LPFG,[18,19] this structure does not need to be processed on a LPFG and has greater flexibility.

2. Experimental setup

2.1. FMF filter

Figure 1 shows a FMFF structure formed by dislocation splicing of a FM-LPFG and a SMF (Corning-28e). The FM-LPFG inscribed the two-mode fiber (TMF) with core/cladding diameters of 19 μm/125 μm, respectively. When the LP_{01} mode passes through the FM-LPFG, most energy of the LP_{01} mode is coupled to the LP_{11} mode, blended with a portion of incompletely converted LP_{01} mode. Due to the different propagation constants of the two modes in the TMF, the phase difference occurs during transmission through the TMF. The two modes interfere at the dislocation splicing point of the TMF and SMF, and the spectral intensity is periodically modulated with respect to the wavelength[20]

$$I = I_1 + I_2 + 2\sqrt{I_1 I_2}\cos(\Delta\phi), \tag{1}$$

where I_1 and I_2 are the transmission LP_{01} and LP_{11} mode intensities in the TMF, respectively. $\Delta\phi$ is the phase difference of the two modes and can be expressed as

$$\Delta\phi = 2\pi\Delta n_{\text{eff}} L/\lambda = 2\pi(n_{\text{eff1}} - n_{\text{eff2}})L/\lambda, \tag{2}$$

where L is the length of the TMF and Δn_{eff} is the mode effective refractive index difference. n_{eff1} and n_{eff2} are the effective refractive indices of the LP_{01} and LP_{11} modes, respectively. The modulation period of the filter can be approximately expressed as[21]

$$\Delta\lambda \approx \lambda^2/\Delta n_{\text{eff}} L. \tag{3}$$

It can be derived from Eqs. (1) and (3) that the extinction ratio (modulation intensity) of the interfered spectrum depends on the intensity ratio between the two modes, and the FSR (modulation period) is related to the TMF length. The longer the TMF length, the smaller the FSR.

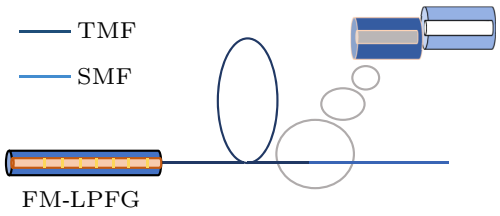


Fig. 1. The FMFF structure diagram.

In the experiments, by changing the dislocation distance between the SMF and TMF cores, the insertion loss of the FMFF and the visibility of the interference spectrum can be tuned. When the TMF length after the FM-LPFG is chosen to be 0.6 m, the transmission spectrum variation of the FMFF with the dislocation distance is shown in Fig. 2. As the dislocation distance increases from 0 μm to 5.5 μm, the corresponding spectrum changes from black to cyan. The experimental results show that the larger the dislocation distance, the higher the spectral visibility of the comb formed by the FMFF. This means that the extinction ratio of the filter in the C-band gradually increases, and the loss gradually decreases. Macroscopically, the transmission spectrum gradually tends to be flat. At the same time, the FSR of this filter remains unchanged. However, when the dislocation distance is further increased, the overall insertion loss of the filter also increases. Therefore, finding a suitable dislocation distance is of great significance for the application of this structure in fiber lasers.

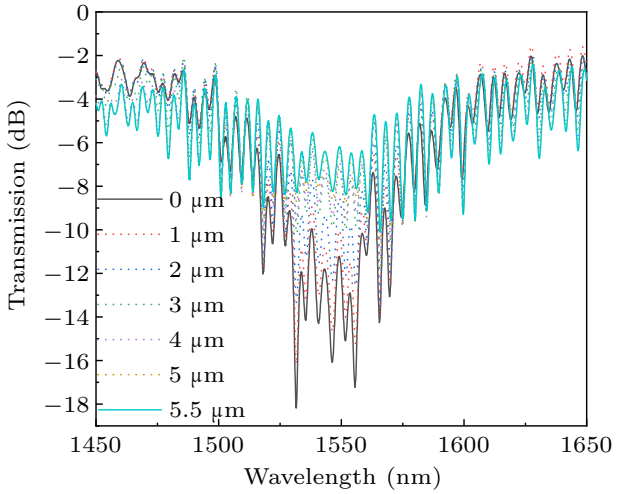


Fig. 2. The transmission spectrum variation of the FMFF with the dislocation distance.

2.2. Laser structure

Wavelength-switchable mode-locked fiber lasers are of great significance for wavelength-division multiplexing (WDM) in optical communications. The schematic diagram of the wavelength-switchable mode-locked fiber laser we built is shown in Fig. 3. The laser resonator is pumped by a 980 nm laser diode (LD) through a 980 nm/1550 nm wavelength division multiplexer (WDM). The laser amplification is completed by the length of 1.4 m EDF, and the EDF dispersion parameter is 69 ps^2/km. A PC is used to adjust the energy balance in the laser cavity and optimize the mode-locking state of the laser cavity. The fiber coupler with 10% output is used to observe the operating state of the laser cavity, mainly measuring the laser working wavelength and temporal pulse output. A semiconductor saturable absorber mirror (SESAM) connected by a fiber optical circulator is used to realize the soliton pulse formation, while reflecting the energy back into the cavity. Here, the fiber circulator not only connects the semiconductor saturable absorption mirror, but also ensures that the laser operates in one direction. The total length of the laser cavity is 11.76 m, of which the SMF length is 9.36 m. The dispersion parameter of the SMF is -22.8 ps^2/km, and the dispersion parameter of the TMF is -26.9 ps^2/km. Therefore, the net dispersion in the laser cavity is -0.1437 ps^2.

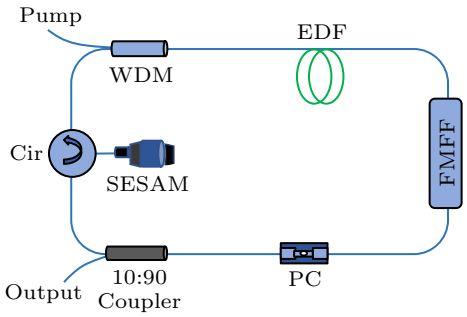


Fig. 3. Laser schematic.

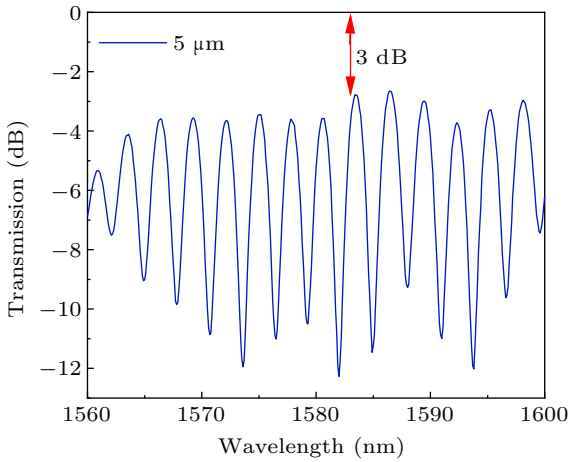


Fig. 4. Filtering spectrum of the FMFF.

In order to obtain a better comb spectrum, the TMF length after the FM-LPFG is set to 1 m, and the formed FMFF is placed in the laser. By optimizing the dislocation distance, the dislocation splicing distance was selected as 5 μm. The transmission spectrum of the structure measured by broadband light source (BLS) is shown in Fig. 4. The filter spectrum has a FSR of 3.2 nm, a loss of 3 dB, and an extinction ratio of up to 9 dB. This periodic modulation spectrum in the laser can cause inhomogeneity in the gain range, thereby realizing multiwavelength laser output.

3. Experimental results and discussion

When the pumping power is lower than the mode-locking power and higher than the laser oscillation threshold power, the laser outputs a CW. When the pump power is 100 mW, the energy is too low to generate a pulse train. By carefully tuning the PC, the lasers obtain single-, dual-, triple-, and quadruple-wavelength outputs. The spectra measured by the optical spectrum analyzer (OSA, YOKOGAWA-AQ6370D) are shown in Fig. 5, respectively. Figure 5 reveals that the wavelength number and peak wavelength of the laser output are switchable. This is the result of a combination of filter-induced longitudinal mode competition and polarization hole burning effect. Figure 5(a) demonstrates the switching of the single wavelength peak from 1562.72 nm to 1574.34 nm with a tunable range of 11.62 nm. The individual wavelength spacing matches the FSR of the FMFF. The switching of the dual wavelength from 1560.08 nm to 1568.18 nm with a tunable range of 8.1 nm is shown in Fig. 5(b). Figure 5(c) demonstrates the switching of the triple-wavelength peaks from 1560.08 nm to 1563.06 nm with a tunable maximum interval of 2.98 nm. Figure 5(d) shows the quadruple-wavelength laser output spectrum at wavelengths of 1562.68 nm, 1565.74 nm, 1568.62 nm, and 1571.48 nm, respectively. The change of the polarization state in the laser cavity, the signal-to-noise ratio (SNR) of the single-wavelength, dual-wavelength, triple-wavelength and quadruple-wavelength lasers formed are greater than 49 dB, 47 dB, 36 dB, and 41 dB, respectively. This is due to the relatively high contrast of the comb-filtered spectrum formed by the FMFF. It is difficult to obtain the quadruple-wavelength laser output shown in Fig. 5(d) due to the intense competition of longitudinal modes. In addition, the stability and tunability of the quadruple-wavelength laser outputs by the laser are relatively weak. The experimental results show that the laser can achieve switchable single-wavelength, dual-wavelength and triple-wavelength output, and quadruple-wavelength laser output.

When the pump power is increased to 130 mW, the working state of the laser is converted from CW to mode-locking state. The OSA measures the spectrum from the output port, as shown in Fig. 6(a). The spectral center wavelength is 1567.72 nm, and the 3 dB bandwidth is 0.049 nm. At the same time, the pulse sequence measured by the oscilloscope

(OSC, RIGOL-DS4054) is shown in Fig. 6(b), and the pulse interval is 58.769 ns. Figure 6(c) shows that in the frequency range of 100 Hz, the measured SNR with a resolution bandwidth (RBW) of 1 Hz is 61 dB. Figure 6(d) shows the radio frequency (RF) spectrum in the 0 GHz–2 GHz range, and it can be observed that the pulse sequence is stable. The pulse repetition frequency is 17.0157 MHz, which is consistent with the theoretical calculation result of cavity length.

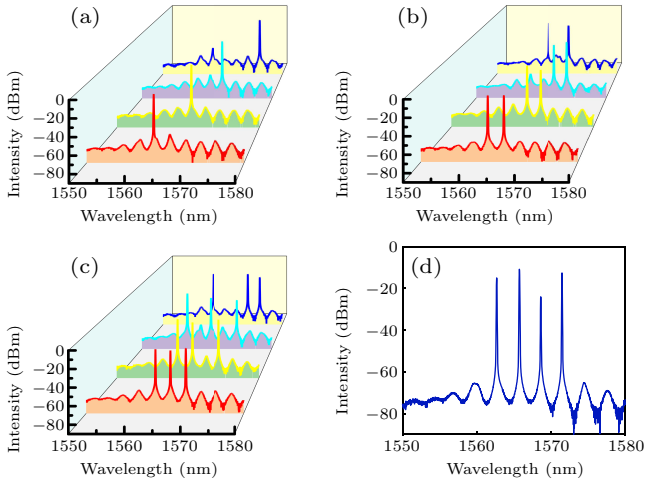


Fig. 5. CW laser output spectra. (a) Single wavelength laser. (b) Dual wavelength laser. (c) Triple-wavelength laser. (d) Quadruple-wavelength laser.

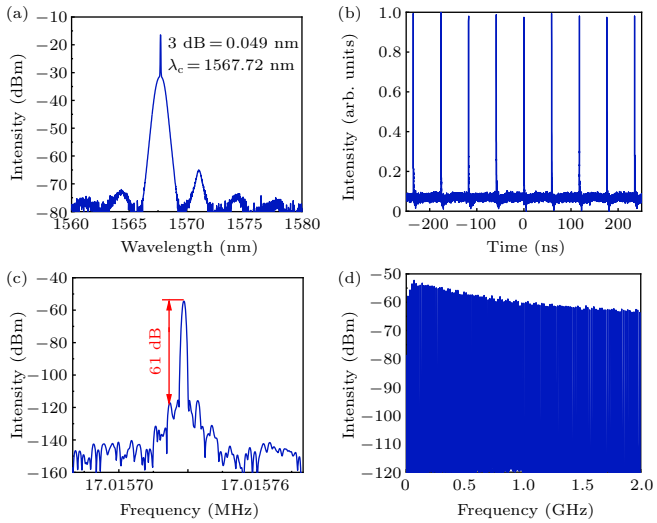


Fig. 6. (a) Output spectrum. (b) Mode-locked pulse sequence. (c) Corresponding RF spectrum in the 100 Hz range. (d) RF spectrum in the 2GHz range.

Under the condition of keeping the pump power unchanged, adjusting the PC changes the polarization state of the light in the cavity, so that the laser can reach a new mode-locking state. At this time, the spectrum analyzer measures the spectrum from the output port as shown in Fig. 7(a). The spectral center wavelength changed from 1567.72 nm to 1571.04 nm, and the 3 dB bandwidth changed to 0.044 nm. The pulse train interval translates to 58.77 ns, as shown in Fig. 7(b). The SNR measured at the resolution of 1 Hz is 61.2 dB. The RF spectra in the 100 Hz and 0 GHz–2 GHz frequency range are shown in Figs. 7(c) and 7(d), respectively. Compared with the soliton pulse at the center wavelength 1567.72 nm, the pulse repetition frequency and the spectral 3 dB bandwidth remain basically unchanged. In this experiment, the SNR of the long wavelength laser pulse is higher than that of the short wavelength laser pulse. The small difference in the interval of the pulse sequence further proves that the repetition rate of the pulse in the laser cavity is related to the working wavelength of the pulse. The pulse has a duration of approximately 57.07 ps at 1567.72 nm, whereas the pulse duration is approximately 63.3 ps when operating at 1571.04 nm. In this syringe-like mode-locked spectrum, the spectral base bandwidth is much larger than the tip bandwidth. The peak pulse width of the soliton spectrum is much smaller than that of the base, because the pump energy is relatively low, and the peak pulse width does not have enough energy broadening.

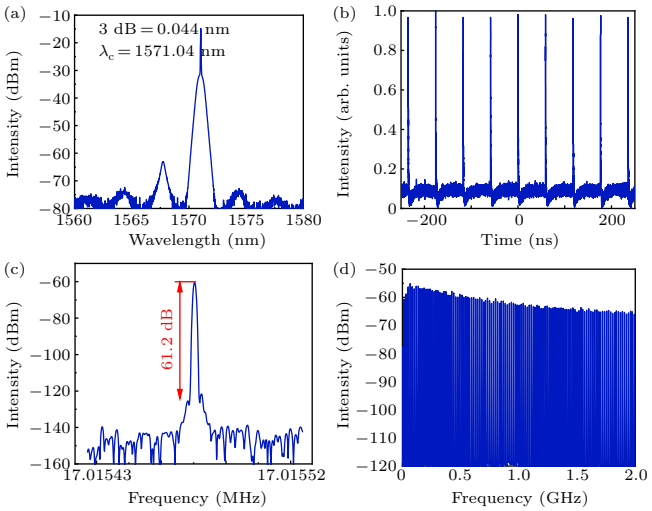


Fig. 7. The new state. (a) Output spectrum. (b) Mode-locked pulse sequence. (c) Corresponding RF spectrum in the 100 Hz range. (d) RF spectrum in the 2 GHz range.

The experimental results also show that when the mode locking is completed in the laser cavity, the tunability of the mode-locked laser wavelength is weaker than that of the continuous laser wavelength. This is because the soliton spectral formation of the mode-locked state is the result of the balance of a series of effects, such as the dispersion effect, the saturable absorption effect of the SESAM, and the Kerr effect.[22] The spectral narrowing caused by FMFF filtering balances with the spectral broadening caused by the self-phase modulation effect in the cavity, leading to the self-uniform evolution of the soliton pulses in the cavity. Keep the polarization state of the laser in the cavity unchanged, gradually increase the energy of the pump light, and measure the energy of the output port as shown in Fig. 8. The efficiency of the laser is 0.454%. The FMFF structure in the experiment can be constructed repeatedly, and different TMF lengths will produce filtering spectra

with different FSR. When the filter spectrum is applied to a fiber lasers, different wavelengths of laser output are produced.

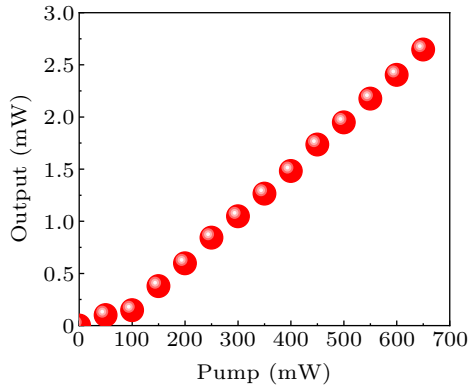


Fig. 8. The relationship between laser output power and pump power.

4. Conclusion

In summary, we have constructed a FMFF by dislocation splicing of a FM-LPFG and a SMF, which has a good comb filtering function. From the all-fiber laser based on the FMFF filtering effect, the generation of switchable single-, dual-, triple-, and quadruple-wavelength continuous light has been achieved. Furthermore, wavelength switchable mode-locked pulses have been obtained with the increased pump power. The wavelength of the output pulses can be switched from 1567.72 nm to 1571.04 nm, with the SNR persisting above 61 dB. The laser has relatively high flexibility and stability, and has potential application prospects in many fields such as high precision optical measurement, optical fiber sensing systems, and optical communication.

Acknowledgments

Project supported by the National Natural Science Foundation of China (Grant Nos. 91950105 and 62175116) and the 1311 talent plan of Nanjing University of Posts and Telecommunications.

References

[1] Wong C Y, Tong F W, Cheng Z Z, Xu K, Chen Y M and Tsang H K 2014 *Appl. Phys. B* **114** 367
[2] Xu M G, Archambault J, Reekie L and Dakin J 1994 *Electron. Lett.* **30** 1085
[3] Yin G L, Lou S Q, Wang X and Han B L 2013 *Laser Phys. Lett.* **10** 125110
[4] Yao Y, Chen X F, Dai Y T and Xie S Z 2006 *IEEE Photonics Technol. Lett.* **18** 187
[5] Zhang C F, Sun J and Jian S S 2013 *Opt. Commun.* **288** 97
[6] Han Y G and Lee S B 2005 *Opt. Express* **13** 10134
[7] Mao X Q, Yan F P, Wang L, Feng S C, Peng J and Jian S S 2009 *Opt. Commun.* **282** 93
[8] Tran T V A, Lee K, Lee S B and Han Y G 2008 *Opt. Express* **16** 1460
[9] Hu S, Zhan L, Song Y J, Li W, Luo S Y and Xia Y X 2005 *IEEE Photonic Technol. Lett.* **17** 1387
[10] Tang M, Jiang Y C, Li H S, Zhao Q, Cao M, Mi Y A, Jian W, Ren W H and Ren G B 2020 *J. Lightwave Technol.* **38** 3745
[11] Sierra-Hernandez J M, Rojas-Laguna R, Vargas-Rodriguez E, Estudillo-Ayala J M, Jauregui-Vazquez D, Guzman-Chavez A D and Zaca-Moran P 2013 *Laser Phys.* **23** 125103
[12] Feng S C, Xu O, Lu S H and Jian S S 2009 *Chin. Phys. Lett.* **26** 064208
[13] Huang L G, Chang P F, Song X B, Peng W H, Zhang W D, Gao F, Bo F, Zhang G Q and Xu J J 2016 *Opt. Express* **24** 2406
[14] Zou H, Ma L, Xiong H, Zhang Y S and Liu C X 2017 *Optoelectron. Lett.* **13** 409
[15] Qi Y H, Kang Z X, Sun J, Ma L, Jin W X, Lian Y D and Jian S S 2016 *Opt. Laser Technol.* **81** 26
[16] Tang M, Jiang Y C, Zhao Q, Cao M, Mi Y A, Jian W, Ren W H and Ren G B 2019 *IEEE Photonic Technol. Lett.* **31** 1623
[17] Liu M, Tang M, Cao M, Mi Y A, Guan P H, Ren W H and Ren G B 2021 *Opt. Commun.* **492** 126964
[18] Liu X S, Zhan L, Lou S Y, Wang Y X and Shen Q S 2011 *J. Lightwave Technol.* **29** 3319
[19] Miao R, Zhang W, Feng X, Zhao J H and Liu X M 2009 *Chin. Phys. Lett.* **26** 074208
[20] Shao M, Qiao X G, Fu H W, Li H D, Zhao J L and Li Y 2014 *Opt. Lasers Eng.* **52** 86
[21] Mao D, Liu X M, Sun Z P, Lu H, Han D D, Wang G X and Wang F Q 2013 *Sci. Rep.* **3** 3223
[22] Gao Q, Du Y Q, He Z W, Mao D and Zhao J L 2021 *J. Lightwave Technol.* **39** 6276